Working group report: Quantum chromodynamics

Coordinator: V RAVINDRAN[9]

Contributors: Pankaj Agrawal[1], Rahul Basu[2], Satyaki Bhattacharya[3], J Blümlein[4], V Del Duca[5], R Harlander[6], D Kosower[7], Prakash Mathews[8] and Anurag Tripathi[9]

[1]Institute of Physics, Sachivalaya Marg, Bhubaneswar 751 005, India
[2]Institute of Mathematical Sciences, CIT Campus, Taramani, Chennai 600 113, India
[3]Delhi University, New Delhi 110 019, India
[4]Deutsches Elecktronen Synchrotron DESY, Zeuthen, Germany
[5]INFN, Turin, Italy
[6]Bergische Universitat Wuppertal, Germany
[7]Saclay, SPhT, France
[8]Saha Institute of Nuclear Physics, 1/AF Bidhan Nagar, Kolkata 700 064, India
[9]Harish Chandra Research Institute, Allahabad 211 019, India
E-mail: ravindra@mri.ernet.in

Abstract. This is the report of the subgroup QCD of Working Group-4 at WHEPP-9. We present the activities that had taken place in the subgroup and report some of the partial results arrived at following the discussion at the working group meetings.

Keywords. Quantum chromodynamics; resummation; extra dimensions; multi-leg.

PACS No. 12.38.-t

1. Introduction

The focus during the working group meetings was mainly on higher-order QCD radiative corrections to processes that are important at hadronic colliders such as Tevatron at Fermilab and LHC at CERN. Both at Tevatron and LHC, the scattering processes are initiated by quarks and gluons that constitute the scattering hadrons. The infra-red safe observables at these colliders factorise into calculable perturbative part and non-perturbative parton distribution functions. The pertubative part is computable in QCD in terms of the strong coupling constant α_s. The leading-order contributions are often very sensitive to renormalisation and factorisation scales. This can lead to large theoretical uncertainties making most of the leading-order predictions unreliable. The higher radiative QCD corrections can only reduce these scale uncertainties. In addition, the corrections could be large in some kinematic regions which can be probed by the experiments. Such large

corrections can be resummed to all orders in the strong coupling constant. These resummed results along with fixed order predictions are almost free of theoretical uncertainties originating from the renormalisation and factorisation scales. The computation of higher-order QCD radiative corrections becomes difficult due to the increasing number of loops and also the large number of external particles at every loop. In addition, the light particles bring in additional complications while evaluating various contributions beyond leading order. There is no single method that can deal with all the processes involving multi-loops, multi-legs and also light particles. Now the task is to identify the process that is phenomenologically important and also require higher-order corrections. And then one has to find a suitable method to compute QCD corrections to them for the physics goal.

2. QCD and extra dimensions

The gauge hierarchy problem has been one of the main motivation for physics beyond the Standard Model (SM). An important question is why the gravity appears weak as compared to the other three interactions of the SM. This apparent weakness has been accounted for either by the existence of large extra spatial dimension ADD model [1] or due to warped extra dimension RS model [2]. In these cases the fundamental Planck scale could be of the order of a TeV providing a possible explanation of the hierarchy. Here, only gravity is allowed to propagate the extra dimensions and the SM fields live in 3-brane. Due to compactification one ends up with Kaluza–Klein modes in four-dimensions, which lead to distinct KK spectrum and their effective interaction with the SM model particles. The experimental signatures of these KK modes have been of intense phenomenological activity. At hadron colliders, it is important to have a precise knowledge of the parton distribution functions (PDFs) [3] to predict production cross-sections of both signals and backgrounds. The PDFs are extracted from global fits to available data in deep inelastic scattering, Drell-Yan and other hadronic processes. Various groups have parametrised the PDFs for a wide range of proton momentum fraction x carried by the parton and for the center-of-mass energy Q^2 at which the process takes place. There are various uncertainties that enter the parametrisation of the PDFs and in addition there are also uncertainties due to unknown higher-order perturbative corrections. It is also important to estimate the uncertainties that come in the PDF distributions. We have looked at the PDF [4] dependence of dilepton pair production at LHC and Tevatron including the gravity effects in the ADD and RS models incorporating the NLO QCD corrections. The PDFs used here are the ALEKHIN, CTEQ, GRV, MRST.

   For both new physics searches and precision SM physics it is essential to understand the uncertainties associated with PDFs. We study to what extent the cross-sections depend on the various PDFs, viz. Alekhin, CTEQ, GRV and MRST. In table 1, we have tabulated the particular PDF that is chosen for the study and also the corresponding $\Lambda_{\rm QCD}$ parameter that is used to determine the strong coupling $\alpha_{\rm s}$. In the case of Alekhin the PDF itself generates the value of $\alpha_{\rm s}$ and is hence not tabulated. We have included all the next-to-leading order corrections to the observables in our study [5,6]. We have looked at various distributions, namely invariant mass, rapidity and angular distributions and also the K-factors.

Quantum chromodynamics

Table 1.

LO		NLO	
PDF	Λ_{QCD} (GeV)	PDF	Λ_{QCD} (GeV)
MRST2001 LO	0.220	MRST2001 NLO	0.323
CTEQ6L	0.326	CTEQ6M	0.326
GRV92LO	0.200	GRV92HO	0.200

In the ADD model, we have chosen $d = 3$ and $M_S = 2$ TeV. In figure 1a the cross-section is plotted as a function of the invariant mass Q of the dilepton at LHC for various PDFs. We see only a mild dependence on the difference in the PDFs. But when plotted for the corresponding K-factor, the PDF dependence is larger for both low and high values of Q (figure 1b). At low Q it is the SM part which is contributing to the K-factor while at high Q it is the beyond SM effects that contribute to the K-factor. At low Q where the K-factor is due to SM part, MRST and CTEQ are similar, while Alekhin and GRV are much smaller. At large Q the K-factor is due to the gravity part and here CTEQ is larger.

For the RS model we have chosen the mass of the first KK mode $M_1 = 1.5$ TeV and the coupling $c_0 = 0.01$. In figure 2a we have plotted invariant mass distribution of the dilepton in the RS model. At the KK mode resonances the cross-section differs from the SM cross-section, but the dependence on the PDFs are very mild. In figure 2b the corresponding K factors are plotted for various PDFs. There is a wide difference in the K-factor, more in the second peak and even off peak where the effect is mainly SM. This may be due to the high Q value that is chosen in the RS case. In this case GRV varies substantially from the rest.

3. Sudakov resummation

In the QCD-improved parton model, the infra-red safe observables, such as hadronic cross-sections can be expandable in terms of perturbatively calculable partonic cross-sections appropriately convoluted with non-perturbative operator matrix elements known as parton distribution functions (PDF). The fixed-order QCD predictions have limitations in applicability due to the presence of various logarithms of kinematical origins. These logarithms become large in some kinematical regions which otherwise can be probed by the experiments. The approach to probe these regions is to resum these logarithms in a closed form [7–9]. Such an approach of resumming a class of large logarithms supplemented with fixed order results can almost cover the entire kinematic region of the phase space. In addition, these threshold corrections are further enhanced when the flux of the incoming partons become large in those regions. In the case of Higgs production through gluon fusion, the gluon flux at small partonic energies becomes large improving the role of threshold corrections. Here, we consider the inclusive cross-sections of hadronic cross-sections such as deep inelastic scattering, DY, Higgs production through gluon fusion and bottom quark annihilation and study the effects of soft gluons that origi-
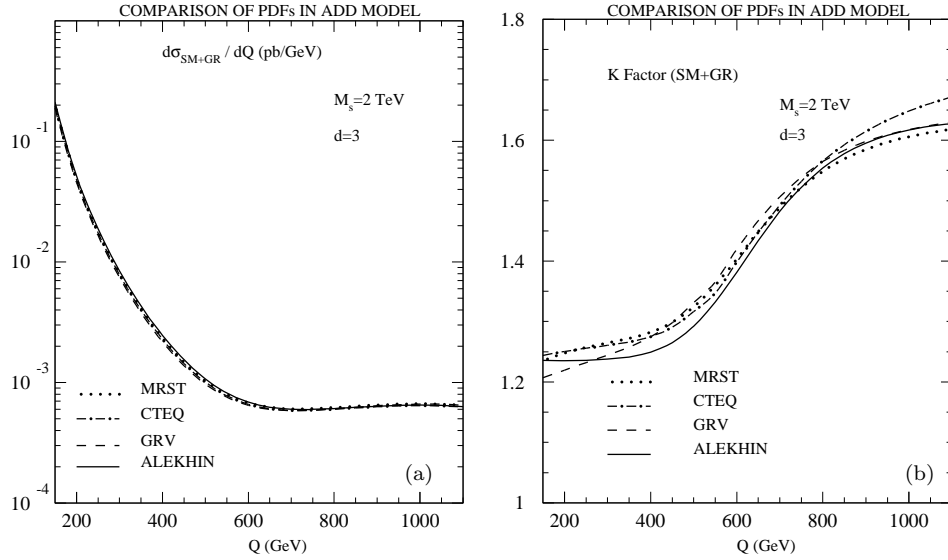
COMPARISON OF PDFs IN ADD MODEL

COMPARISON OF PDFs IN ADD MODEL

$d\sigma_{SM+GR}$ / dQ (pb/GeV)

M_s=2 TeV

d=3

K Factor (SM+GR)

M_s=2 TeV

d=3

..... MRST
−·−·− CTEQ
− − − GRV
——— ALEKHIN

(a)

..... MRST
−·−·− CTEQ
− − − GRV
——— ALEKHIN

(b)

Q (GeV)

Q (GeV)

Figure 1. (**a**) Invariant mass distribution of the dilepton pair for ADD model with different PDFs to NLO in QCD. (**b**) The corresponding K-factor for various PDFs.
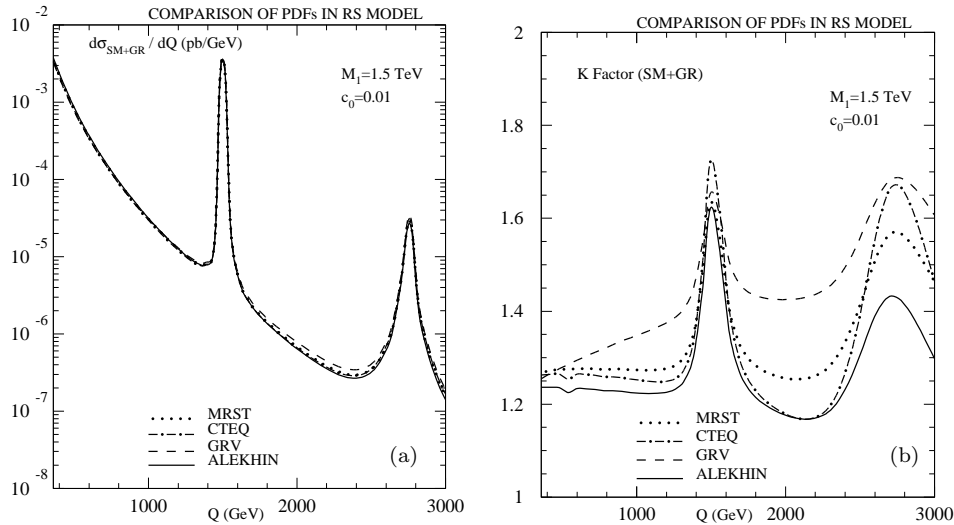
COMPARISON OF PDFs IN RS MODEL

COMPARISON OF PDFs IN RS MODEL

$d\sigma_{SM+GR}$ / dQ (pb/GeV)

M_1=1.5 TeV
c_0=0.01

K Factor (SM+GR)

M_1=1.5 TeV
c_0=0.01

..... MRST
−·−·− CTEQ
− − − GRV
——— ALEKHIN

(a)

..... MRST
−·−·− CTEQ
− − − GRV
——— ALEKHIN

(b)

Q (GeV)

Q (GeV)

Figure 2. (**a**) The invariant mass distribution of dilepton pair production at LHC in the RS model for various PDFs. (**b**) The corresponding K-factor for various PDFs.

nate in the threshold region of the phase space. We extend this approach to bottom quark energy distribution in Higgs decay as well as to hadroproduction in l^+l^- annihilation. In these processes, large logarithms are generated when the gluons that are emitted from the incoming/outgoing partons become soft. We find that the

soft distribution function of Higgs production can be obtained entirely from the DY process by a simple multiplication of the colour factor C_A/C_F [10]. This is applicable to the other important process, namely Higgs production through bottom quark annihilation. Using the soft distribution functions extracted from DY, and the form factor of the Yukawa coupling of Higgs to bottom quarks, we can now predict soft plus virtual part of the Higgs production through bottom quark annihilation beyond NNLO with the same accuracy that DY process and the gluon fusion to Higgs are known [11]. This generalises our earlier approach to include any infra-red safe inclusive cross-section. We can determine the threshold exponents $D_i^{\rm I}$ up to three loop level for DY and Higgs productions using our resummed soft distribution functions. Similarly, using the results available for the DIS, we can determine threshold-enhanced contributions to bottom quark energy distribution in Higgs decay as well as to hadroproduction in l^+l^- annihilation [12]. This is achieved using the appropriate crossing relations between these two different type of processes. We can also provide all order proof which establishes the relation between soft distribution functions and threshold exponents in the standard Mellin space resummation approach [8,9]. We have used renormalisation group (RG) invariance, mass factorisation and Sudakov resummation of QCD amplitudes as the guiding principles.

Since we are only interested in the effect of soft gluons, the infra-red safe observable can be obtained by adding soft part of the cross-sections with the virtual contributions and performing mass factorisation using appropriate counter terms. We call this infra-red safe combination a 'soft plus virtual' (SV) part of the cross-section. The soft plus virtual part of the cross-section ($\Delta_{I,P}^{\rm SV}(z,q^2,\mu_R^2,\mu_F^2)$) after mass factorisation is found to be

$$\Delta_{I,P}^{\rm SV}(z,q^2,\mu_R^2,\mu_F^2) = \mathcal{C}\exp(\Psi_P^{\rm I}(z,q^2,\mu_R^2,\mu_F^2,\varepsilon))|_{\varepsilon=0}, \tag{1}$$

where $\Psi_P^{\rm I}(z,q^2,\mu_R^2,\mu_F^2,\varepsilon)$ is a finite distribution. The subscript $P={\rm S}$ for Drell-Yan (DY) and Higgs productions and $P={\rm SJ}$ for deep inelastic scattering. The symbol S stands for 'soft' and SJ stands for 'soft plus jet'. For DY and DIS, $I=q$ (quark/anti-quark) and for Higgs production through gluon fusion, $I=g$ (gluon) and for bottom quark annihilation to Higgs boson, $I=b$ (bottom quark). Here $\Psi_P^{\rm I}(z,q^2,\mu_R^2,\mu_F^2,\varepsilon)$ is computed in $4+\varepsilon$ dimensions.

$$\begin{aligned}\Psi_P^{\rm I}(z,q^2,\mu_R^2,\mu_F^2,\varepsilon) = &(\ln(Z^{\rm I}(\hat{a}_{\rm s},\mu_R^2,\mu^2,\varepsilon))^2 + \ln|\hat{F}^{\rm I}(\hat{a}_{\rm s},Q^2,\mu^2,\varepsilon)|^2)\\ &\times \delta(1-z) + 2\Phi_P^{\rm I}(\hat{a}_{\rm s},q^2,\mu^2,z,\varepsilon)\\ &-2m\mathcal{C}\ln\Gamma_{II}(\hat{a}_{\rm s},\mu^2,\mu_F^2,z,\varepsilon),\end{aligned} \tag{2}$$

where $I=q,g,b$ and $m=1$ for DY and Higgs productions and $m=1/2$ for DIS. The symbol '$\mathcal{C}$' means convolution. Here we encounter only distributions of the kind $\delta(1-z)$ and $\mathcal{D}_i$, where

$$\mathcal{D}_i = \left[\frac{\ln^i(1-z)}{(1-z)}\right]_+ \quad i=0,1,\ldots. \tag{3}$$

Here $\hat{F}^{\rm I}$ are the form factors, $Z^{\rm I}$ are the operator renormalisation constants and Γ_{II} are the diagonal entries of the Altarelli–Parisi splitting functions. The soft distribution functions $\Phi^{\rm I}$ satisfy Sudakov-type differential equation:

V Ravindran

$$
q^2 \frac{\mathrm{d}}{\mathrm{d}q^2} \Phi_P^{\mathrm{I}}(\hat{a}_{\mathrm{s}}, q^2, \mu^2, z, \varepsilon) = \frac{1}{2} \Bigg[\bar{K}_P^{\mathrm{I}} \left(\hat{a}_{\mathrm{s}}, \frac{\mu_R^2}{\mu^2}, z, \varepsilon \right)
$$
$$
+ \bar{G}_P^{\mathrm{I}} \left(\hat{a}_{\mathrm{s}}, \frac{q^2}{\mu_R^2}, \frac{\mu_R^2}{\mu^2}, z, \varepsilon \right) \Bigg], \tag{4}
$$

where the constants $\bar{K}_P^{\mathrm{I}}$ contain all the singular terms and $\bar{G}_P^{\mathrm{I}}$s are finite functions of ε. Also, $\Phi_P^{\mathrm{I}}(\hat{a}_{\mathrm{s}}, q^2, \mu^2, z)$ satisfy the renormalisation group equation:

$$
\mu_R^2 \frac{\mathrm{d}}{\mathrm{d}\mu_R^2} \Phi_P^{\mathrm{I}}(\hat{a}_{\mathrm{s}}, q^2, \mu^2, z, \varepsilon) = 0. \tag{5}
$$

Solving, we can express the soft distribution function (for any m) as

$$
\Phi_P^{\mathrm{I}}(\hat{a}_{\mathrm{s}}, q^2, \mu^2, z, \varepsilon) = \Bigg(\frac{m}{1-z} \Bigg\{ \int_{\mu_R^2}^{q^2(1-z)^{2m}\delta_P} \frac{\mathrm{d}\lambda^2}{\lambda^2} A_I \left(a_{\mathrm{s}}(\lambda^2) \right)
$$
$$
+ \bar{G}_P^{\mathrm{I}} \left(a_{\mathrm{s}} \left(q^2(1-z)^{2m}\delta_P \right), \varepsilon \right) \Bigg\} \Bigg)_+
$$
$$
+ \delta(1-z) \sum_{i=1}^{\infty} \hat{a}_{\mathrm{s}}^i \left(\frac{q^2 \delta_P}{\mu^2} \right)^{i(\varepsilon/2)} S_\varepsilon^i \, \hat{\phi}_P^{\mathrm{I},(i)}(\varepsilon)
$$
$$
+ \left(\frac{m}{1-z} \right)_+ \sum_{i=1}^{\infty} \hat{a}_{\mathrm{s}}^i \left(\frac{\mu_R^2}{\mu^2} \right)^{i(\varepsilon/2)} S_\varepsilon^i \, \bar{K}^{\mathrm{I},(i)}(\varepsilon), \tag{6}
$$

where $\delta_P = (-1)^{2m}$ and

$$
\bar{G}_P^{\mathrm{I}} \left(a_{\mathrm{s}} \left(q^2(1-z)^{2m}\delta_P \right), \varepsilon \right) = \sum_{i=1}^{\infty} \hat{a}_{\mathrm{s}}^i \left(\frac{q^2(1-z)^{2m}\delta_P}{\mu^2} \right)^{i(\varepsilon/2)} S_\varepsilon^i \bar{G}_P^{\mathrm{I},(i)}(\varepsilon). \tag{7}
$$

For $m = 1$, that is, for DY and Higgs production, we can easily identify $G_{\mathrm{S}}^{\mathrm{I}}(a_{\mathrm{s}}(q^2(1-z)^2), \varepsilon)$ with the threshold exponent $D^{\mathrm{I}}(a_{\mathrm{s}}(q^2(1-z)^2))$:

$$
D^{\mathrm{I}}(a_{\mathrm{s}}(q^2(1-z)^2)) = \sum_{i=1}^{\infty} a_{\mathrm{s}}^i(q^2(1-z)^2) D_i^{\mathrm{I}}
$$
$$
= 2\bar{G}_{\mathrm{S}}^{\mathrm{I}}(a_{\mathrm{s}}(q^2(1-z)^2), \varepsilon)|_{\varepsilon=0}. \tag{8}
$$

We find

$$
D_i^{\mathrm{I}} = 2\bar{\mathcal{G}}_{\mathrm{S},i}^{\mathrm{I}}(\varepsilon = 0). \tag{9}
$$

For $m = 1/2$, that is, for DIS, we identify $G_{\mathrm{SJ}}^{\mathrm{I}}(a_{\mathrm{s}}(Q^2(1-z)), \varepsilon)$ with the threshold exponent $B_{\mathrm{DIS}}^{\mathrm{I}} \left(a_{\mathrm{s}} \left(Q^2(1-z) \right) \right)$:

Quantum chromodynamics

$$B_{\text{DIS}}^{\text{I}}(a_{\text{s}}(Q^2(1-z))) = \sum_{i=1}^{\infty} a_{\text{s}}^i(Q^2(1-z))B_{\text{DIS},i}^{\text{I}}$$
$$= \bar{G}_{\text{SJ}}^{\text{I}}(a_{\text{s}}(Q^2(1-z)),\varepsilon)\big|_{\varepsilon=0}. \tag{10}$$

We find

$$B_{\text{DIS},i}^{\text{I}} = \bar{\mathcal{G}}_{\text{SJ},i}^{\text{I}}(\varepsilon = 0). \tag{11}$$

Using the resummed expression given in eq. (1) and the known exponents, we can obtain the results for $\Delta_{\text{I},P}^{\text{SV},(i)}$ for DY, Higgs production and DIS.

We have also studied the bottom quark energy distribution in Higgs decay and also the hadroproduction in l^+l^- annihilation using a similar approach and extended the similar all order proof which establishes the relation between soft plus jet distribution functions and the threshold resummation exponents. This way, we can demonstrate the usefulness of this approach to derive higher-order threshold enhanced corrections for any infra-red safe decay distributions. Here the soft distribution function can be obtained entirely from Φ^{I} given in eq. (6) by replacing δ_P by $|\delta_P|$ and choosing $m = 1/2$. This is due to the crossing relation between DIS and decay distributions. Due to this simplification, we find the threshold exponent which appears in the resummed results for the decay distributions satisfy

$$B_{\text{decay}}^{\text{I}}(a_{\text{s}}(q^2(1-z))) = \sum_{i=1}^{\infty} a_{\text{s}}^i(q^2(1-z))B_{\text{decay},i}^{\text{I}}$$
$$= \bar{G}_{\text{SJ}}^{\text{I}}(a_{\text{s}}(q^2(1-z)),\varepsilon)\big|_{\varepsilon=0} \tag{12}$$

giving

$$B_{\text{decay},i}^{\text{I}} = \bar{\mathcal{G}}_{\text{SJ},i}^{\text{I}}(\varepsilon = 0). \tag{13}$$

4. Production of two vector bosons and a jet through gluon fusion

As colliders cross new energy and luminosity frontiers, there will be opportunity to test the Standard Model in new domains. In particular, one can observe the processes, that were not accessible earlier. One class of such processes that would be accessible at the LHC is: $gg \to VV'g$. Here V or V' could be an appropriate combination of γ, W or Z^0 vector bosons. The process $gg \to \gamma\gamma g$ has been studied in the past. We are working on the calculation of the remaining processes. These processes will produce large number of events at the LHC. These processes are also backgrounds to the Higgs boson (and similar particles of the Standard Model extensions) and techni-particles. In the Standard Model these processes occur at the one loop through pentagon and box type diagrams. In particular, we focus on the process $gg \to Z^0 Z^0 g$. The strategy we are following for this calculation is described below.

For the process $gg \to Z^0 Z^0 g$, there are 42 diagrams: 24 pentagon type and 18 box type. First we obtain the analytical expressions for the helicity amplitude of

V Ravindran

one generic pentagon type and one generic box type diagram using FORM. We manipulate this amplitude further using FORM and rewrite it in terms of tensor loop integrals. Most complicated integral is a five-tensor pentagon type. This amplitude is then converted to a FORTRAN routine. By appropriate permutations of the external momenta, we can obtain the amplitudes for all the diagrams. Next step in the computation is to calculate the tensor integrals. We use the techniques of Oldenborgh and Vermaseren to convert the tensor integrals into scalar integral. These scalar integrals can then be computed analytically by standard techniques. In this computation, we neglect the mass of the quark in the loop. The individual pieces in the amplitude have UV singularities, mass singularities and IR singularities. However, the final amplitude is finite. The cancellation of singularities is an important check on the calculation.

The final step in the calculation is to compute amplitude numerically, take the square of the modulus, and perform phase space integrals to obtain the cross-section and the distributions. This final code is expected to be slow. As in an earlier calculation, we shall use PVM/MPI for the parallel computing of the cross-section and the distributions.

5. A proposal for studying multiple cone algorithm for isolation of photons at LHC

Studying the production of prompt photons is going to be of great interest for the experiments at the Large Hadron Collider (LHC). While the Higgs boson decaying to two photons has been identified as one of the most important discovery channels for a light ($\sim$90 to $\sim$150 GeV) Higgs, measuring rate of prompt photon production from parton–parton hard scattering is going to be an interesting measurement in itself, as a probe of QCD. The rate measurement of single prompt photon+jet production, for example, should be able to provide useful constraints on the gluon PDF. Given the high rate of direct photon production, physics with photon will be possible even at the very beginning of the LHC data-taking. However, one crucial issue in the study of direct photons is the effective suppression of processes where either a jet particle like π^0, ρ or η fakes a photon in the electromagnetic calorimeter (ECAL) or a process where there is a high p_T photon coming from fragmentation. π^0's are copiously produced in jets and decay to two photons with almost 100% branching fraction [13], other neutral mesons ρ, η, η' and K_S can also produce electromagnetic shower consistent with a photon. At the LHC these particles produced inside high p_T jets will typically be so boosted that the decay photons will make a very small opening angle and often will hit the same crystal or adjacent crystals of the ECAL and will appear like a single photon. A di-jet event with one jet having such a fake photon form the most serious background to single prompt photon + jet events. To suppress this background, demanding the photon candidate to be isolated, i.e. demanding that there should not be any substantial hadronic activity around the direction of photons is needed. Isolation algorithms used in the experiments at hadron colliders require that the energy deposits in both the hadron and electromagnetic calorimeters and the number of charged particle tracks in the tracker, in a single cone around the direction of the candidate photon be less than a threshold. Typical cone size used is $\Delta R = (\Delta\eta^2 + \Delta\phi^2)^{0.5} =\sim 0.4$.

However, in calculation of the theoretical cross-sections if such a cut is applied, it leads to fragmentation function dependence of the cross-section because it allows soft emissions collinear to the direction of the photon. If one attempts to eliminate collinear configurations, cancellation of infra-red singularities is spoiled. An alternative is to define a concentric set of isolation cones around the photon direction with required threshold energies decreasing as a function of the cone radius in such a manner that in the limit of cone radius going to zero the energy allowed in the isolation cone is zero [14].

This algorithm has not been tried out in any experimental direct photon search so far. The major experimental difficulty in implementing this algorithm comes from the fact that the granularity of the calorimeter (crystal size) limits the number of concentric cones that can be defined inside $R = \sim 0.4$ and because very small energy requirement within the cones cannot be measured reliably. The CMS experiment at the Large Hadron Collider (LHC) is a multipurpose detector that has a crystal-based electromagnetic calorimeter (ECAL) with excellent granularity and energy resolution [15] and provides a good opportunity for attempting an implementation of this idea. The CMS experiment has done detailed Monte Carlo study of photon isolation variables in the context of Higgs search in the gamma–gamma decay mode [17].

In several full detector simulations, typical cone sizes for isolation of 0.3 to 0.4 have been used for ECAL-based isolation. In the barrel region of the CMS ECAL the extent of each crystal in both η and ϕ directions are 0.0175 and cone radius of 0.4 corresponds to almost 23 crystals whereas almost 97% of the photon energy is contained in a 5×5 crystal matrix.

However, there is one issue which one should be careful about while developing multi-cone isolation algorithm. In the CMS there is about 0.4 to 0.6 radiation length (depending on η) tracker material present in front of the ECAL and there is a large probability of the photons converting in the tracker volume. In this case the shower produced by the resulting electron–positron pair and the bremsstrahlung photons emitted by them is much more spread out in the ECAL and is irregular in shape. In this case one has to use a clustering to estimate the energy and angle of the photon and use this information to subtract the energy of the photon from the total energy in the isolation cone.

Such clustering (referred to as superclustering in the CMS reconstruction software) algorithms have already been developed and carefully studied with detailed GEANT4-based Monte Carlo simulation of detector effects [16]. One can make use of this algorithm in the case of photons which have converted early enough in the tracker.

Hence we propose the following: In the study of inclusive prompt diphoton or single photon channel demand the transverse energy ($E_{\mathrm{T}}^{\mathrm{cone_1}}$) found in the ECAL in a cone of radius $R1 = 0.4$ in addition to the E_{T} of the candidate photon should be less than $E_{\mathrm{T}}^{\mathrm{max_1}} = 2$ GeV. In addition demand that E_{T} in a cone of radius $R2 = 0.2$ ($E_{\mathrm{T}}^{\mathrm{cone_2}}$) in addition to E_{T} of photon be less than $E_{\mathrm{T}}^{\mathrm{max_2}} = 0.5$ GeV and match with the rate under the same isolation criteria estimated from a theoretical NLO level program, e.g. Diphox [18].

V Ravindran

To estimate the photon energy we will use the energy in a 5×5 crystal matrix for unconverted (or late converted) photons and for early converted photons we will use the supercluster energy.

As a next step one can try increasing the number of cones and similar multi cone isolation algorithms in hadron calorimeter or tracker-based isolation algorithms and study the performance of this algorithm in rejecting nonisolated photons.

One should be able to test this algorithm on the LHC direct photon data in the very early days of data-taking and match the direct photon rate with theoretical prediction at NLO accuracy in a consistent way.

References

[1] N Arkani-Hamed, S Dimopoulos and G Dvali, *Phys. Lett.* **B249**, 263 (1998)
    I Antoniadis, N Arkani-Hamed, S Dimopoulos and G Dvali, *Phys. Lett.* **B436**, 257 (1998)
[2] L Randall and R Sundrum, *Phys. Rev. Lett.* **83**, 3370 (1999)
[3] M Dittmar *et al*, *LHC workshop*, arXiv:hep-ph/0511119
[4] M C Kumar, P Mathews and V Ravindran, *Distributions in ADD and RS*, arXiv:hep-ph/0604135
[5] P Mathews, V Ravindran, K Sridhar and W L van Neerven, *Nucl. Phys.* **B713**, 333 (2005), arXiv:hep-ph/0411018
[6] P Mathews, V Ravindran and K Sridhar, *J. High Energy Phys.* **0510**, 031 (2005), arXiv:hep-ph/0506158
[7] V V Sudakov, *Sov. Phys. JETP* **3**, 65 (1956); *Zh. Eksp. Teor. Fiz.* **30**, 87 (1956)
[8] G Sterman, *Nucl. Phys.* **B281**, 310 (1987)
[9] S Catani and L Trentadue, *Nucl. Phys.* **B327**, 323 (1989)
[10] V Ravindran, arXiv:hep-ph/0512249
[11] V Ravindran, *Processes in QCD*, arXiv:hep-ph/0603041
[12] J Blumlein and V Ravindran, *Hadroproduction in l^+l^-*, arXiv:hep-ph/0605011
[13] Particle Data Group: S Eidelman *et al*, *Phys. Lett.* **B592**, 1 (2004) and 2005 partial update for edition 2005; http://pdg.lbl.gov
[14] Stefano Frixione, hep-ph 98011442, 29 Jan 1998
[15] Tracker Technical Design Report, CERN/LHCC 98-6 (15 April 1998)
     ECAL Technical Design Report, CERN/LHCC 97-33 (15 December 1997)
     For HCAL resolution, see e.g. Powel de Barbaro, CMS/CR 2000/015 (2000)
     For muon system summary, see e.g. P Giacomelli, *The CMS Muon Detector*, VCI 2001 Conference
[16] E Meschi *et al*, CMS Note 2001/034 (25 June 2001)
[17] See e.g. M Pieri *et al*, CMS Note 2006/112 (9 June 2006)
[18] See http://wwwlapp.in2p3.fr/lapth/$PHOX_FAMILY$/diphox.html and references therein